Materials Science-Poland, *Vol. 27*, *No. 4/1*, *2009*

Synthesis and characterization of nanoscale $Bi_2Cu_{0.1}V_{0.9}O_{5.35}$ powders by solution-based chemical methods

M. GUO[1], H. DENG[2], P. YANG[1*]

[1]Key Laboratory of Polar Materials and Devices, Department of Electronics, East China Normal University, Shanghai 200241, China

[2]Instrumental Analysis and Research Center, Institute of Materials, Shanghai University, 99 Shangda Rd, Shanghai 200444, China

Nanocrystalline $Bi_2Cu_{0.1}V_{0.9}O_{5.35}$ (BCVO) powders were synthesized by solution-based chemical methods. Materials have been characterized by the thermogravimetric analysis, X-ray diffraction, and scanning/transmission electron microscopy. The sintering temperatures to complete phase transition are above 330 °C, 320 °C and 470 °C for the primary powders obtained by the sol-gel technique, an ethylenediaminetetra acetate–citrate combustion gel route and a modified reversing titration co-precipitation method (RP), respectively, which were much lower than the 600 °C required by conventional solid state method (SS). The powders synthesized by EC with 2 wt. % of surfactant, polyethylene glycol PEG 4000 have rather a narrow size distribution, within 30–50 nm, and as the PEG 4000 content increases, they form agglomerates irregular in shapes. In RP the optimal concentration of PEG 4000 is about 5 wt. % and the average grain size of the sample is 20 nm. The modified reaction in homogeneous solutions can be controlled to produce uniform BCVO nanoparticles.

Key words: *ionic conduction; nanoscale powders; solution-based chemical methods; surfactant*

1. Introduction

$Bi_2Me_xV_{1-x}O_{5.5-3x/2}$ (BMVO) materials derived from the parent structure of ferroelectric bismuth vanadate $Bi_2VO_{5.5}$, where vanadium is partially replaced by different divalent or trivalent metal ions (Me), exhibit stable, high oxide-ion conductivity of the γ-phase at room temperature [1]. Potential applications have been developed for solid oxide fuel cells (SOFC), oxygen separation, oxygen sensing and oxidation membranes [2, 3]. The conductivity of BMVO is dependent on the characteristics of the material

*Corresponding author, e-mail: pxyang@ee.ecnu.edu.cn

[2, 4] such as particle size, morphology, purity, chemical composition, and phase, which are greatly affected by the preparation technique. The conventional way, namely diffusion-limited solid-state reaction by mixing oxide with repeatedly grinding/milling to synthesize the material, has some inherent disadvantages, including broad particle size distribution, chemical inhomogeneity, large particle size and introduction of impurities during milling/grinding, due to the high temperature required to obtain the target phase [1, 5, 6]. While the solution-based chemical methods such as sol-gel technique [7], co-precipitation [8], citrate combustion [9] and EDTA chelating [10] processes can provide homogeneously mixed reactants in atomic scale under relatively mild conditions.

On the other hand, owing to the difference in acidity of ions with different charges, the chemical reactivity of Bi^{3+} and V^{5+} source precursors is different, leading to low homogeneity of Bi–V oxide precursors. Good control over the properties of the precursor can overcome the above problem and nanocrystalline powders can thereby be obtained. The solution-based techniques show a great potential for the preparation of homogeneous mixed oxide gels.

Of all the BMVO materials, the highest conductivities have been exhibited by copper substituted bismuth vanadates $Bi_2Cu_xV_{1-x}O_{5.5-3x/2}$. It is reported that high-temperature tetragonal γ-phase is stable at room temperature for copper substitution of $0.07 \leq x \leq 0.20$ [11, 12]. The optimum conductivity is considered to be at $x = 0.1$, which corresponds to BCVO. The materials have been synthesized by conventional solid-state reaction method [11,12], which takes a long time and requires a relatively high temperature. This paper presents, for the first time, a systematic investigation into the synthesis of tetragonal nanocrystalline BCVO powders via solution-based methods, including modified sol-gel, ethylenediamine tetraacetate (EDTA)–citrate combustion gel and reversing titration precipitation. For comparison, BCVO powders were also prepared by a solid-state reaction at 600 °C. In addition, the adsorption of a surfactant such as polyethylene glycol (PEG) on the particle surface can prevent particle–particle aggregation due to steric hindrance effect [13–15], and therefore the effect of PEG on the BCVO was also investigated.

2. Experimental

$Bi(NO_3)_3 \cdot 5H_2O$ (AR), $Cu(NO_3)_3 \cdot 3H_2O$ (AR), NH_4VO_3 (AR), HNO_3 (65% w/w), ammonia, tetramethylammonium hydroxide (TMAH, 25% w/w aqueous solution, electronic grade), EDTA, polyethylene glycol PEG 4000 (average molecular weight equal to 4000) were used as supplied without further purification.

Firstly, a modified sol-gel technique (SG) was performed to synthesize BCVO. 20 mmol of $Bi(NO_3)_3 \cdot 5H_2O$ was dissolved in 10 cm^3 of 4 M HNO_3, and then 1 mmol of $Cu(NO_3)_3 \cdot 3H_2O$ was added into the solution. 9 mmol of NH_4VO_3 was dissolved into 20 cm^3 of 25% (w/w) aqueous solution of TMAH, which is a strong organic alkali,

instead of the conventional inorganic alkali. These two solutions were mixed and continuously stirred at room temperature for 0.5 h. The solution was quantitatively transferred to form 0.2 M green sol, and then the gel was formed overnight. The gel was dried completely at 80 °C and then milled. The powders were sintered in air at the given temperature in the range 300–600 °C for 4 h.

Secondly, the material was synthesized by the EDTA–citrate combustion gel method (EC). The same stoichiometric amounts of $Bi(NO_3)_3{\cdot}5H_2O$, $Cu(NO_3)_3{\cdot}3H_2O$ and NH_4VO_3 as above were dissolved in EDTA–$NH_3{\cdot}H_2O$ aqueous solution with continuously stirring at 60 °C, and then a proper amount of citric acid was added. 0 wt. %, 2 wt. %, 5 wt. % and 10 wt. % of PEG 4000 was added to the solutions. The solutions were concentrated at 80 °C to produce gels. The dark yellow fluffy products were obtained after the evaporation of water and then they were crushed. The samples were sintered in air at a given temperature in the range 300–600 °C for 4 h.

Thirdly, the material was synthesized by a modified reversing titration co-precipitation method (RP). $Bi(NO_3)_3{\cdot}5H_2O$ and $Cu(NO_3)_3{\cdot}3H_2O$ in the same molar ratio of 20:1 as above were dissolved in dilute nitric acid with different amounts of surfactant PEG 4000 (0, 2, 5 and 10 wt. %), NH_4VO_3 in stoichiometric amount was dissolved in 500 cm^3 of 1.26 M solution of ammonia, and then the mixed solution of $Bi(NO_3)_3$ and $Cu(NO_3)_3$ was added into NH_4VO_3 solution dropwise with mild stirring at 60 °C. The obtained precipitate was aged at 60 °C for 2 h, and then was washed with deionized water and subsequently with ethanol. The filtered samples were allowed to dry at 80 °C to get yellow material. The primary material was sintered in air at a given temperature in the range 300–600 °C for 4 h.

Finally, the material was synthesized by a conventional solid-state reaction method (SS) as comparison. A stoichiometric mixture of $Bi(NO_3)_3{\cdot}5H_2O$, $Cu(NO_3)_3{\cdot}3H_2O$ and NH_4VO_3 was milled with a mortar, and then dried at 80 °C. The mixture was sintered at 600 °C for 4 h.

Thermogravimetric analysis and differential thermal analysis (TG/DTA) of the powders were performed on a TGA 851e/SF/1100 thermogravimeter at the scan rate of 10 °C/min in air from ambient temperature to 850 °C. X-ray diffraction (XRD) analysis was carried out using a Rigaku D/max2200 diffractometer. Scanning electron microscopy (SEM) analysis was performed using a JEOL JSM-6700 scanning electron microscope. Transmission electron microscopy (TEM) analysis was performed using a JEOL-2000FX transmission electron microscope.

3. Results and discussion

The results of TGA analyses on the as-synthesized dry gels by SG are shown in Fig. 1. In the temperature range 25–120 °C, the mass of the sample decreased, which was consistent with the loss of water. The persistence of water/OH groups associated with oxide materials at high temperatures has been noted in another study [16]. Loss of water is attributed primarily to physisorbed water until approximately 120 °C.

Above this temperature, the total weight loss, of about 38 %, in the temperature range of 120–330 °C resulted from condensation of the surface hydroxyl group or evaporation of chemisorbed water and decomposition of the inorganic/organic composites such as the nitrates, the residual NH_4^+ and organic residues. There was a significant large exothermic peak centred at 330 °C in the DTA curve, corresponding the transition from α to γ phase [17]. In addition, there was no significant peak beyond 330 °C, indicating that the sintering temperature above 330 °C is possibly adequate for the as-synthesized dry gels to complete phase transition.

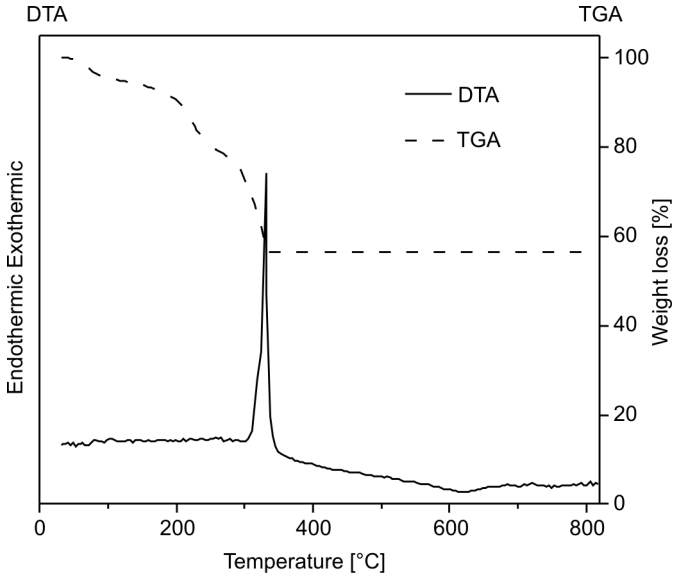

Fig. 1. TGA/DTA patterns of the as-synthesized dry gels prepared by SG

The XRD patterns of the samples obtained by SG after sintering at 300–600 °C for 4 h are shown in Fig. 2a. Phase transition is dependent on the sintering temperature. Tetragonal γ-phase of the parent compound $Bi_2VO_{5.5}$ was observed, indicating that it was stable at room temperature by the partial substitution of Cu for V ions [6]. In the sol-gel process, as evidenced from DTA/TGA patterns in Fig. 1, the crystallization of BCVO gel precursor started at 300 °C as seen in Fig. 2a. But at 300 °C, the phase of $BiVO_4$ also existed, as marked by a cross in Fig. 2a, and it vanished at 400 °C. The peaks of γ-phase $Bi_2VO_{5.5}$ peaks as marked by filled diamonds in Fig. 2a, which were sharp and distinct, indicate a higher degree of crystallinity of the sample. For comparison, the XRD pattern of the sample prepared by SS is shown in Fig. 2b. Some traces of impurity corresponding to $BiVO_4$ are observed after the sample was sintered at 600 °C, and is consistent with previous papers [6, 18]. This indicates that the sintering temperature in the SG process is 300 °C lower than that in conventional solid state methods, where the presence of BCVO phase was observed above 600 °C. We think

that the exothermic decomposition of the gel might provide enough heat to the crystallization of BCVO, and thus reduces the sintering temperature.

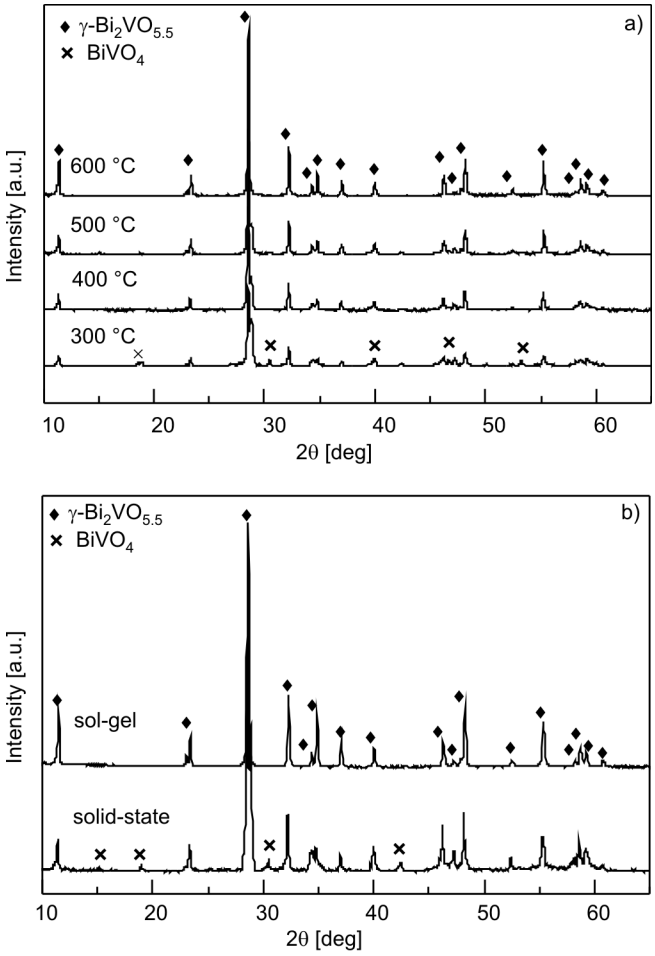

Fig. 2. XRD patterns of the samples prepared by SG after heating at 300–600 °C for 4 h (a) and XRD patterns of the samples prepared by SG and by SS after heating at 600 °C for 4 h (b)

On the other hand, the peak intensities in Fig. 2a increased with the sintering temperature. The average crystallite size of the BCVO powders after heating at 400 °C was about 50 nm at (103) reflection estimated by the Debye–Scherrer formula [17]. The calculated lattice parameters a and c, and cell volume V in powders were 0.3929 nm, 1.5487 nm and 0.23910 nm^3, respectively. These values are consistent with standard values of lattice parameters a = 0.3935 nm, c = 1.5476 nm, and V = 0.23968 nm^3.

The primary powders prepared by SG were brown-yellow, while the calcined powders were bright yellow, consistent with the colour of BCVO. Figure 3a shows the SEM image of the powders after heating at 600 °C.

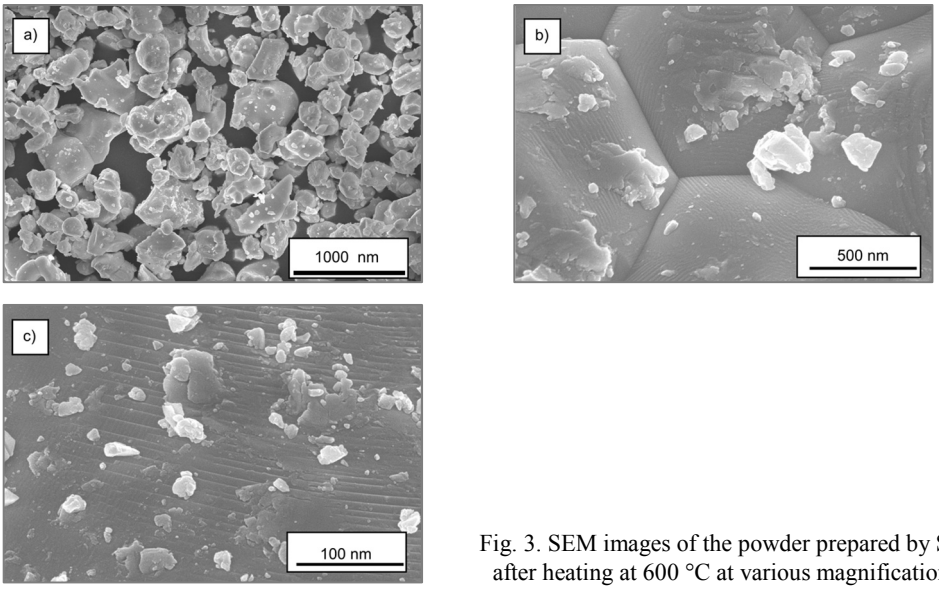

Fig. 3. SEM images of the powder prepared by SG after heating at 600 °C at various magnifications

The particles exhibit a range of sizes and the smallest one was about 200 nm. While the average crystallite size estimated from the XRD analysis of the material was about 50 nm, the actual particle sizes are significantly larger. The extent of aggregation of these particles requires further investigation. The particles have a hexagon-like appearance at the edges observed from the SEM image at high magnification in Fig. 3b. Furthermore, there is a small quantity of small particles adhering to the surface of the large grains in Fig. 3b, indicating the inhomogeneous distribution and the agglomeration of the small particles in the sample. At higher magnification, the terrace-like appearance in Fig. 3c is a possible evidence for a layered structure of the material.

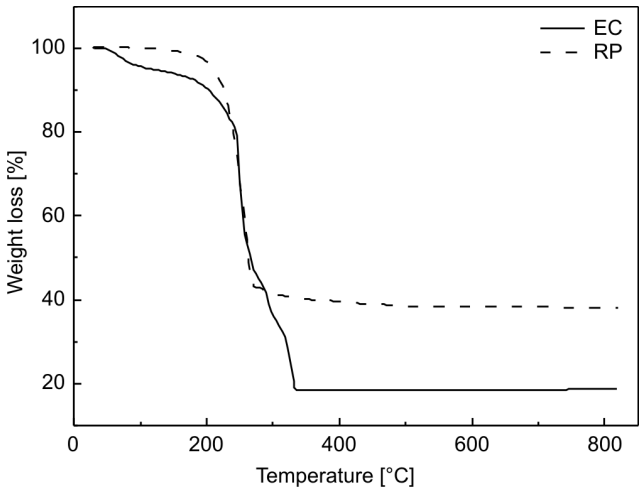

Fig. 4. TGA curves of the samples prepared by EC and RP with 5 wt. % of PEG 4000

The effect of surfactants was explored in order to reduce the particle–particle aggregation and thus reduce the grain size. EC and RP synthesis routes with various amounts of PEG 4000 were investigated. TGA analysis was performed on the primary products prepared by EC and RP with 5 wt. % of PEG 4000, and the results are shown in Fig. 4. Similar to that of the samples prepared by SG (Fig. 1), the weight loss in the temperature range 25–200 °C is attributed to loss of water. Significant weight losses between 200 and 320 °C for the sample fabricated by EC and between 200 and 270 °C for the sample synthesized by RP mainly result from the decomposition of inorganic/organic residues, as well as the decomposition of the surfactant. The total weight loss of the sample obtained by RP was lower than that by EC, indicating a lower content of organic molecules in primary powders obtained by RP. No weight loss occurred for the samples obtained by EC over 320 °C, suggesting that surfactant in the samples could be completely removed at this temperature and the sintering temperature above it is possibly adequate for the sample to complete phase transition. A slight weight loss of the sample made by RP in the temperature range 270–470 °C will be discussed later, together with the XRD results. The temperature of complete phase transition of BCVO fabricated by these three solution-based routes is significantly lower than that of the solid state reaction [19].

The XRD patterns of primary powders added with 0 wt. %, 2 wt. %, 5 wt. % and 10 wt. % of PEG 4000 are shown in Fig. 5. The powders were partially crystalline and the identification of peaks was very difficult due to the doublets of monoclinic and tetragonal $BiVO_4$. In addition, the crystallization was better for the sample with 2 wt. % PEG 4000 for EC and 5 wt. % PEG 4000 for RP compared with the samples with other amounts of PEG 4000 (Fig. 5). However, in order to determine the optimum content of PEG 4000, it is still necessary to examine, via electron microscope images, its effect on dispersions.

The primary samples prepared by EC with 2 wt. % of PEG 4000 were sintered in the temperature range 300–600 °C and their XRD analysis data are shown in Fig. 6. Tetragonal $Bi_2VO_{5.5}$, as marked by filled diamonds and the intermediate phase, $BiVO_4$, as marked by crosses in Fig. 6, were detected for the sample after heating at 300 °C, while the intermediate phase completely disappeared and only tetragonal $Bi_2VO_{5.5}$ was observed for the sample after heating at 400 °C. This is consistent with TGA analysis as shown in Fig. 4, where the mass of the samples was stable above 320 °C in EC. After heating at 500 °C, well-crystallized γ-phase was formed for the samples. When the sintering temperature increased to 600 °C, the peaks became sharper.

The primary samples prepared by RP with 5 wt. % of PEG 4000 were also heated in the temperature range 300–600 °C and the results of their XRD analyses are shown in Fig. 7. Two phases, tetragonal $Bi_2VO_{5.5}$ and the intermediate phase $BiVO_4$, were also observed for the sample after heating at 300 °C and 400 °C, while the intermediate phase completely vanished and only tetragonal $Bi_2VO_{5.5}$ existed at 500 °C. The change of phases from $BiVO_4$ to $Bi_2VO_{5.5}$ (i.e., $BiV_{0.5}O_{2.75}$) causes the

mass loss of the sample due to the evaporation of oxygen in order to maintain the electric charge neutrality, which might explain a slight weight loss seen in the TGA pattern in the temperature range of 270–470 °C (Fig. 4). Compared with XRD analysis of the sample obtained by EC, the required sintering temperature for phase transition increased for the sample obtained by RP, which is consistent with the TGA analysis shown in Fig. 4, where the mass of samples was stable above 320 °C for the EC samples, and above 470 °C for the RP samples. Similarly, peaks became sharper when the sintering temperature increased to 600 °C.

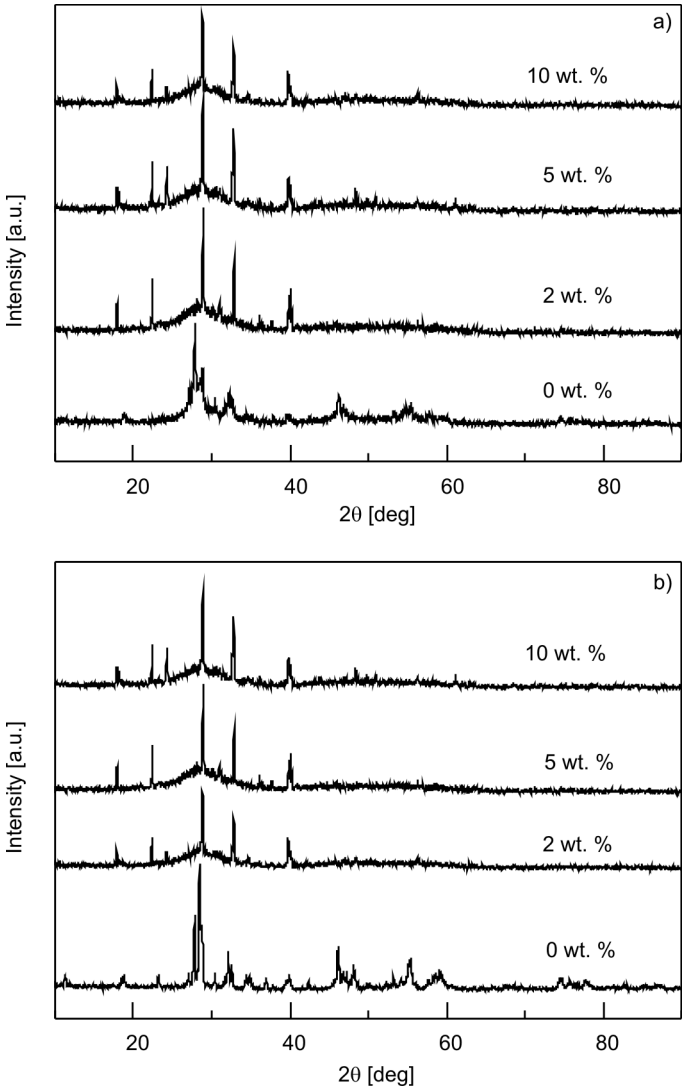

Fig. 5. XRD patterns of the samples with various contents of PEG 4000 prepared by EC (a) and by RP (b)

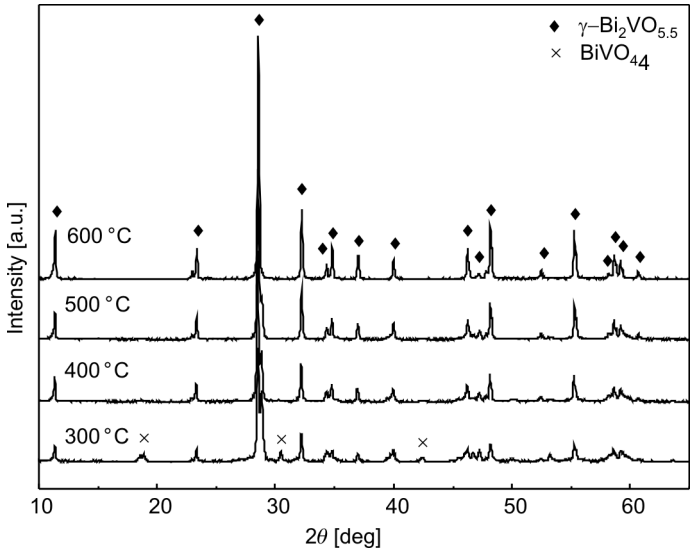

Fig. 6. XRD patterns of the samples prepared by EC with 2 wt. % of PEG 4000 after heating at 300–600 °C for 4 h

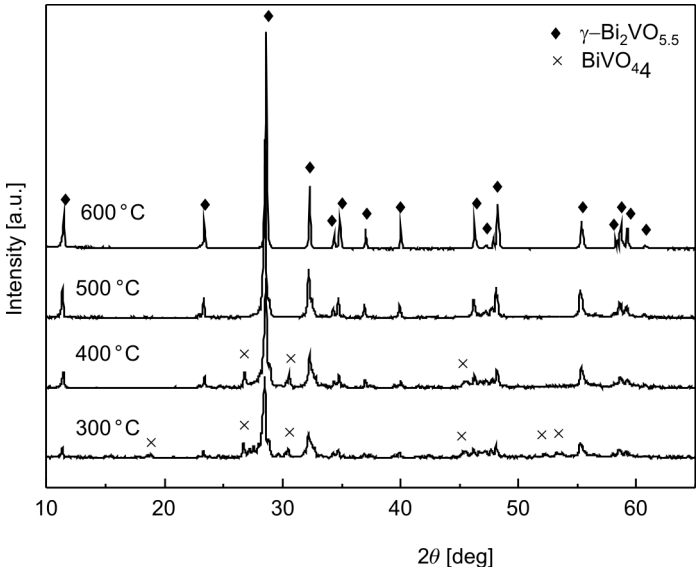

Fig. 7. XRD patterns of the samples prepared by RP with 5 wt. % of PEG 4000 after heating at 300–600 °C for 4 h

In order to investigate the morphology and the particle sizes of the samples with various amounts of PEG 4000 after heating at 500 °C prepared by EC and RP, TEM analyses were performed (Figs. 8 and 9). The particles with 2 wt. % of PEG 4000 have rather narrow size distribution with a slight accumulation phenomenon, and they are spherical. Their sizes are in the range of 30–50 nm (Fig. 8b). The highly agglomerated

products with 5 and 10 wt. % of PEG 4000 were dominated by nanoparticles with irregular shapes (Fig. 8c, d). This suggests that BCVO grains are less uniform and the sizes become larger when the concentration of PEG 4000 increases. The formation of aggregates comprising primary spherical nanoparticles could clearly be observed.

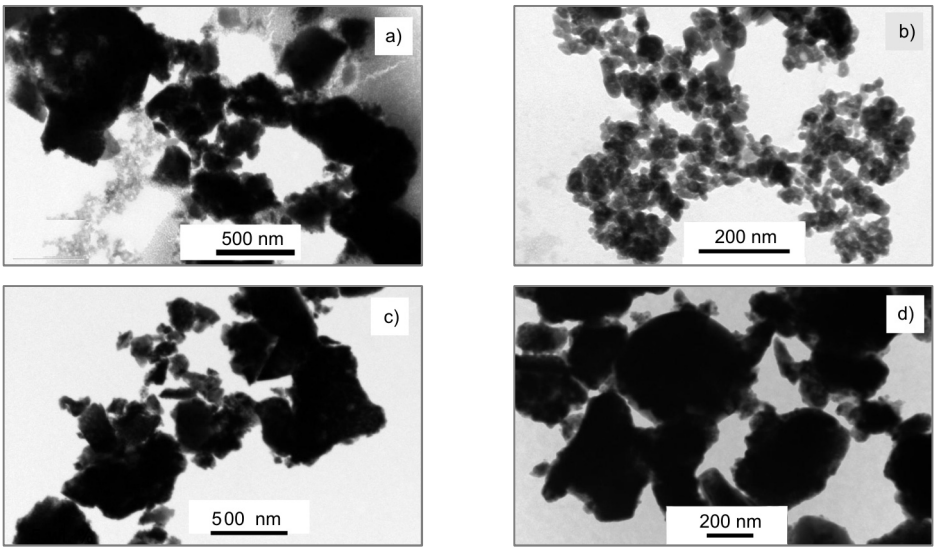

Fig. 8. TEM images of the powder prepared by EC after heating at 500 °C with various amounts of PEG 4000: a) 0 wt. %, b) 2 wt. %, c) 5 wt. %, d) 10 wt. %

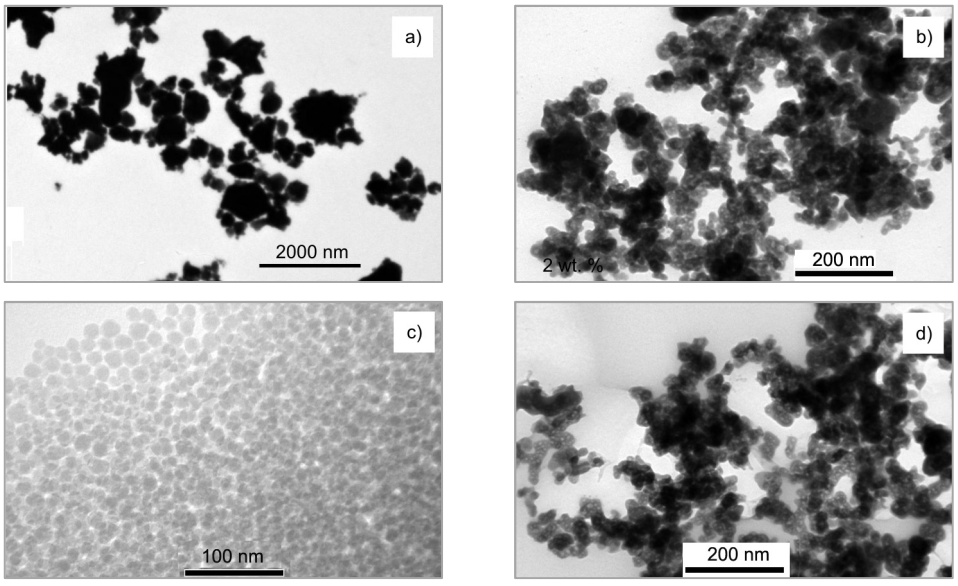

Fig. 9. TEM images of the powder prepared by RP after heating at 500 °C with various amounts of PEG 4000: a) 0 wt. %, b) 2 wt. %, c) 5 wt. %, d) 10 wt. %

However, the samples with 2, 5 and 10 wt. % of PEG 4000 prepared by RP at 500 °C were composed of uniform spherical nanoparticles, as shown in Fig. 9b–d, suggesting that the powders made by RP are much smaller than those made by EC. Adsorption of citrate species, in the EC case, on preferential crystal planes may easily lead to aggregation. The optimum concentration of PEG 4000 is about 5 wt. % in RP and the average grain size of the sample was 20 nm. Figures 9b, d show that the particles aggregated into some flocks, which could be attributed to the shortage and excess of PEG 4000 to coat the precursor with the increase of the nuclei when 2 and 10 wt. % of PEG 4000, respectively, were added. We also note that the morphology and the particle size of the samples with PEG 4000 prepared by SG have no obvious change compared with the primary pure material.

Monodispersed particles are favourable to be formed in solution when the rate of nucleation is much higher than that of the particle growth. The particles of the samples fabricated by SG have no interaction of steric hindrance without surfactant and tend to agglomerate, and therefore the final particles have large grain size, as shown in Fig. 3. In the EC and RP cases, PEG may be adsorbed preferably on the sol particles and keeps them separated in the solution with a polymeric long chain molecule to provide steric hindrance, slowing down the diffusion speed of solutes to the crystal surface of the as-formed nuclei, which ensure that the diffusion process becomes the rate-control step during the crystal growth. The modified reaction in homogeneous solutions can be controlled to produce the most highly uniform BCVO nanoparticles.

4. Conclusions

Nanocrystalline BCVO powders were prepared by the solution-based chemical methods. The sintering temperatures to complete phase transition are above 330 °C, 320 °C and 470 °C for the primary powders made by SG, EC and RP, respectively. Samples prepared by SG, EC and RP contain $BiVO_4$ and γ-$Bi_2VO_{5.5}$ after heating at 300–400 °C, and only γ-$Bi_2VO_{5.5}$ exists above 400–500 °C. The effects of surfactant PEG 4000 on the microstructures of the powders depend on the synthesis routes. The particles in powders obtained by EC with 2 wt. % of PEG 4000 have rather a narrow size distribution, within 30–50 nm, irregular shapes and, as the PEG 4000 content increases, they become more and more highly agglomerated. However, the optimum concentration of PEG 4000 is about 5 wt. % in RP and the average grain size of the sample is 20 nm. A shortage or excess of PEG 4000 can cause the particles to aggregate. In the EC and RP prepared samples, the diffusion process becomes the rate-control step during the crystal growth due to PEG slowing down the diffusion speed of solutes to the crystal surface of the as-formed nuclei. Uniform BCVO nanoparticles can be obtained by controlling the modified reaction in homogeneous solutions.

Acknowledgement

This work was supported by the National Natural Science Foundation of China (60677022), Science Foundation (Research Fund) for Excellent Youth Scholars of Shanghai Municipal Education Commission,

the Key Basic Research Program of Science and Technology Commission of Shanghai Municipality (07JC14018), the State Key Basic Research Program of China (2007CB924902), the Shanghai Leading Academic Discipline Project (B411) and the Ph.D Program Scholarship Fund of ECNU2008 (Project No. 20080051).

References

[1] LAZURE S., VERNOCHET C., VANNIER R.N., NOWOGROCKI G., MAIRESSE G., Solid State Ionics, 90 (1996), 117.
[2] STEIL M.C., FOULETIER J., KLEITZ M., LABRUNE P., J. Eur. Ceram. Soc., 19 (1999), 815.
[3] GOODENOUGH J.B., Nature, 404 (2000), 821.
[4] PRASAD K.V.R., VARMA K.B.R., J. Mater. Sci., 29 (1994), 2691.
[5] EVANS I.R., TAO S.W., IRVINE J.T.S., HOWARD J.A.K., Chem. Mater., 14 (2002), 3700.
[6] CHO H., SAKAI G., SHIMANOE K., Sens. Actuators B, 108 (2005), 335.
[7] PELL J.W., YING J.Y., LOYE H.C., Mater. Lett., 25 (1995), 117.
[8] BHATTACHARYA A.K., MALLICK K.K., THOMAS P.A., Solid State Commun., 91(1994), 357.
[9] ALIFANTI M., BAPS B., BLANGENOIS N., NAUD J., GRANGE P., DELMON B., Chem. Mater., 15 (2003), 395.
[10] WULLENS H., LEROY D., DEVILLERS M., Int. J. Inorg. Mater., 3 (2001), 309.
[11] ABRAHAM F., BOIVIN J.C., MAIRESSE G., NOWOGROCKI G., Solid State Ionics, 40–41 (1990), 934.
[12] ANNE M., BACMANN M., PERNOT E., ABRAHAM F., MAIRESSE G., STROBEL P., Physica B, 180–181 (1992), 621.
[13] CHEN Z., YAN Y., Phys. B, 392 (2007), 1.
[14] WANG X., WANG M., SONG H., DING B., Mater. Lett., 60 (2006), 2261.
[15] ABDULLAH M., OKUYAMA K., LENGGORO I.W., TAYA S., J. Non-Cryst. Solid., 351 (2005), 697.
[16] TOLEDO-ANTONIO J.A., GUTIÉRREZ-BAEZ R., SEBASTIAN P.J., VÁZQUEZ A.J., Solid State Chem., 174 (2003), 241.
[17] NIMAT R.K., BETTY C.A., PAWAR S.H., Appl. Surface Sci., 253 (2006), 2702.
[18] PAYDAR M.H., HADIAN A.M., SHIAMNOE K., YAMAZOE N., J. Eur. Ceram. Soc., 21 (2001), 1825.
[19] YAREMCHENKO A.A., AVDEEV M.V., KHARTON V., KOVALEVSKY A.Y., NAUMOVICH E.N., MARQUES F.M.B., Mater. Chem. Phys., 77 (2002), 552.

Received 22 August 2008
Revised 8 March 2009